Open issues on the structural performances of concrete beams reinforced with FRP (Fiber Reinforced Polymers) rebars.

Maria Antonietta Aiello* and Luciano Ombres**

*Department of Innovation Engineering, University of Salento, Italy
** Department of Civil Engineering, University of Calabria, Italy

Outline

1. *Introduction*
2. *Experimental investigation*
3. *Test results*
4. *Modeling*
5. *Open issues*
6. *Conclusions*

1. Introduction

1.1. Overview

1.2. Objectives and Methodology

1.1. Overview

The widespread state of degradation of reinforced concrete structures is the main problem facing the scientific community.



The use of fiber-reinforced composite materials bars in place of or in combination with traditional steel bars represents one of the most innovative technological solutions for concrete structures, particularly those exposed to aggressive environments, due to their attractive advantages.

1. *High strength;*
2. *High corrosion resistance;*
3. *They are not heat conductors;*
4. *Invisibility to magnetic field;*
5. *Lightness;*
6. *Fast and easy application.*

1.1. Overview

HOWEVER
there are still numerous and not yet fully resolved issues related to the mechanical behavior of concrete structures reinforced with FRP-bars.

One of the relevant aspects is their serviceability behavior in terms of deformability and cracking evolution. It is well known that structures reinforced with FRP bars are generally more deformable than similar structures reinforced with steel bars.

The linear elastic behavior of FRP bars may not guarantee adequate ductility requirements for the structures.

It should be pointed out that the bond between FRP bars and concrete varies as a function of numerous parameters, both geometrical and mechanical.

1.2. Objectives and Methodology

Based on the knowledge gained and with reference to the current state of the art, the issues related to deformability and ductility of concrete elements reinforced with FRP bars are critically analyzed and discussed in this paper.

The analysis is conducted both from an experimental point of view and by an analytical approach aiming to evaluate deflections and cracking phenomenon.

The experimental results are compared with analytical predictions and with predictions developed on the basis of some available codes (ACI, EC2, JSCE).

2. Experimental investigation

2.1. Materials

2.2. Test set-up

2.1. Materials

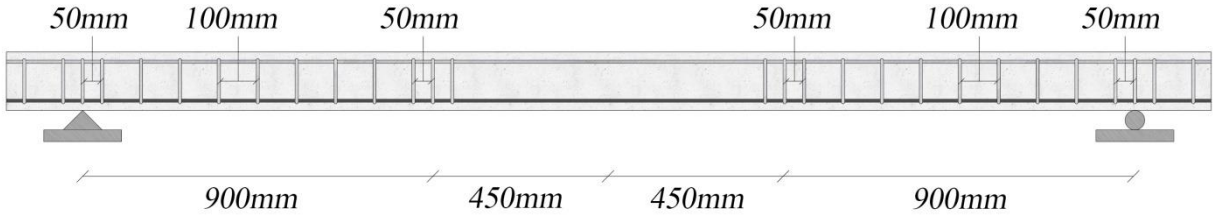

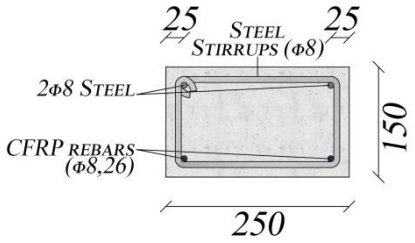

Five beams were reinforced in tension with Carbon FRP bars while steel bars were used in compression and steel stirrups were used as transversal reinforcement.

The beams were 3,000 mm (1181,1 in) long and had a rectangular cross section 250 mm (9,84 in) wide and 150 mm (5,90 in) deep.

Transversal reinforcements composed of steel stirrups with 8-mm (0,315 in) diameter spaced 100 mm (0,394 in) between the loading points and the supports and 50 mm (1,97 in) at the supports and near the loading points.

2.1. Materials

The average values of the concrete compressive and tensile strength were 30,6 MPa (4437 psi) and 2.86 MPa (414.7 psi), respectively.

The average yield strength of steel bars (fy) was 542 MPa (78590 psi).

CFRP bars were 8,26 mm (0,325 in) in diameter, grain covered and helically wounded with carbon fibers.
Average values of the measured tensile strength, elastic modulus and ultimate tensile strain were 2401 MPa (348 ksi), 129 GPa (18676 ksi) and 1.87%, respectively.

The FRP reinforcement ratio ($\rho_f=A_f/b_d$) is reported in Table1.

Table 1. Details of the tested beams

Specimen	Number of FRP bars	A_f (mm^2)	A'_s (mm^2)	ρ_f (x 10^4)
CB-2-1	2	107.12	100.00	28.57
CB-2-2	2	107.12	100.00	28.57
CB-3-1	3	160.68	100.00	42.85
CB-6-1	6	321.35	100.00	85.69
CB-7-1	7	374.91	100.00	99.98

1 mm^2=0.00155 in^2

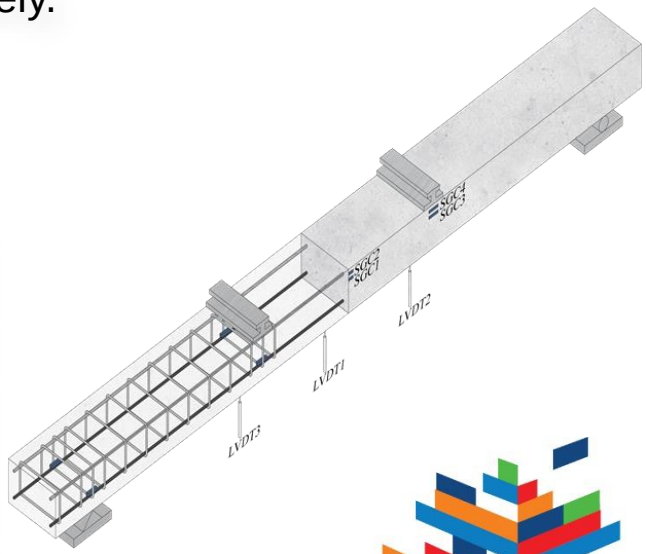

2.2. Test set-up

A four-point bending test was utilized and beams were tested under quasi-static loading conditions up to failure.

Tests were conducted in machine stroke control; the load was applied with a load rate of 40 N/s (9 lbf/s).

- Vertical deflections were measured by three Linear Variable Transducers (LVDTs);
- Electrical strain gauge were bonded to the compressed concrete (gauge length 50 mm);
- The strains of the CFRP bars were measured by electrical strain gauges (gauge length 10 mm);
- Graduate magnifying lens were used to measure crack widths at different load levels.

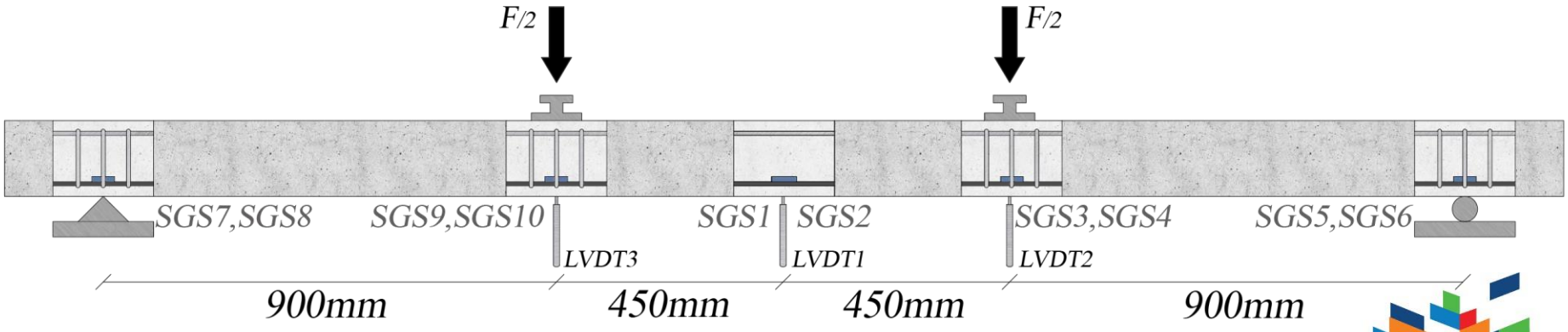

3. Test results

3.1. Failure modes

3.2. Load-deflection curves

3.3. Moment-curvature diagrams

3.4. Ductility

3.5. Crack width and crack spacing

3.1. Failure modes

A shear failure occurred in CB-7-1 beam; the failure finally occurred by concrete crushing at the loading point (*Figure b*).

The remaining beams exhibited the typical flexural behavior; the failure of the beams occurred due to crushing of the compressed concrete *(Figure a*).

The different failure mode observed in the CB-7-1 beam is related to the high reinforcement ratio.


Figura a


Figura b

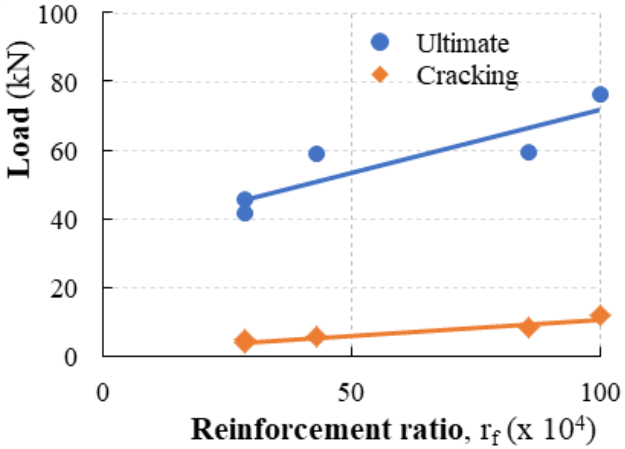

Table 2. Results of tests

Specimen	Cracking load, F_{cr} (kN)	Ultimate load, F_u (kN)	Ultimate mid-span deflection, η (mm)	Ultimate curvature at the mid-span section χ (1/mm)x 10^4	k_s (Nm^2)	DF
CB-2-1	4,90	45,76	91,65	1,1500	1750	7,33
CB-2-2	3,99	41,67	92,05	0,8576	1872	3,96
CB-3-1	5,79	58,75	90,48	0,9586	2382	4,69
CB-6-1	8,39	65,84	78,15	0,9066	2692	4,53
CB-7-1	11,78	76,34	69,57	0,7745	4144	3,77

1 N=0.225 lbf; 1 mm= 0.0394 in

3.2. Load-deflection curves

An almost bilinear curve describes the response of the tested beams.
It is well-known that FRP reinforced concrete beams are more deformable than steel reinforced concrete ones.

The figures evidence two significant aspects of the behavior of CFRP reinforced concrete beams:

- the reduction of the ultimate deflection;
- the increase of the beam stiffness with the increase of the reinforcement ratio.

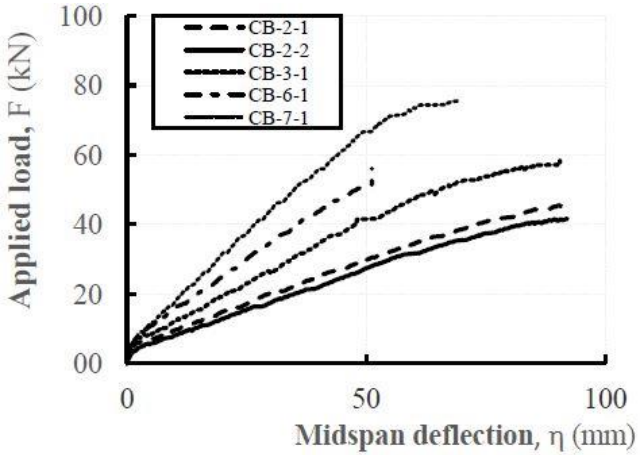

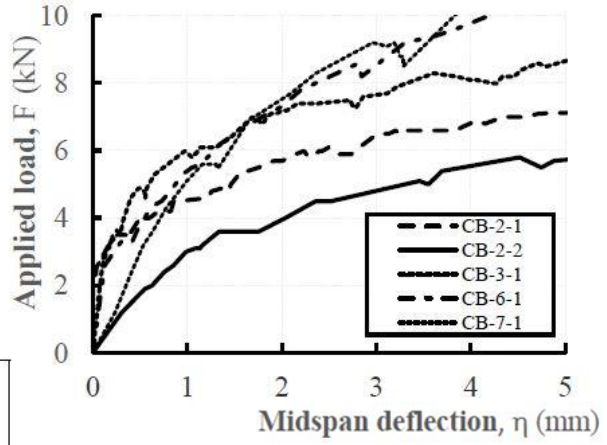

Table 2. Results of tests

Specimen	Cracking load, F_{cr} (kN)	Ultimate load, F_u (kN)	Ultimate mid-span deflection, η (mm)	Ultimate curvature at the mid-span section χ (1/mm)x 10^4	k_s (Nm^2)	DF
CB-2-1	4,90	45,76	91,65	1,1500	1750	7,33
CB-2-2	3,99	41,67	92,05	0,8576	1872	3,96
CB-3-1	5,79	58,75	90,48	0,9586	2382	4,69
CB-6-1	8,39	65,84	78,15	0,9066	2692	4,53
CB-7-1	11,78	76,34	69,57	0,7745	4144	3,77

1 N=0.225 lbf; 1 mm= 0.0394 in

3.3. Moment-curvature diagrams

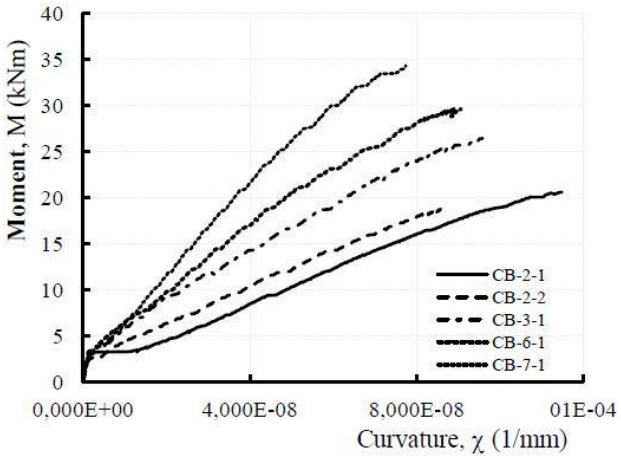

The curvature values were determined as $\chi=(\varepsilon_{cmax}+\varepsilon_{FRP})/d$.

The bending moment was evaluated as $M=(F\cdot a)/2$ being F the total load and a=900 mm (35,43 in) the shear span.

Likewise with load-deflection curves, moment-curvature diagrams show a reduction in deformability as the reinforcement ratio increases.

The values of the flexural stiffness, $k_s=M/\chi$, evaluated with reference to the post-cracking stage are also reported.

Table 2. Results of tests

Specimen	Cracking load, F_{cr} (kN)	Ultimate load, F_u (kN)	Ultimate mid-span deflection, η (mm)	Ultimate curvature at the mid-span section χ (1/mm)x 10^4	k_s (Nm^2)	DF
CB-2-1	4,90	45,76	91,65	1,1500	1750	7,33
CB-2-2	3,99	41,67	92,05	0,8576	1872	3,96
CB-3-1	5,79	58,75	90,48	0,9586	2382	4,69
CB-6-1	8,39	65,84	78,15	0,9066	2692	4,53
CB-7-1	11,78	76,34	69,57	0,7745	4144	3,77

1 N=0.225 lbf; 1 mm= 0.0394 in

3.4. Ductility

The ductility of tested beams was determined through the Deformability Factor. The energy values are evaluated as the area under the moment curvature diagrams. The limit curvature value was conventionally assumed equal to 0,005/d rad/mm [4] being d the effective depth of the beam's cross-section.

3.5. Crack width and crack spacing

Crack widths increase as the reinforcement ratio decreases. This is an expected result being it typical of steel reinforced concrete beams.

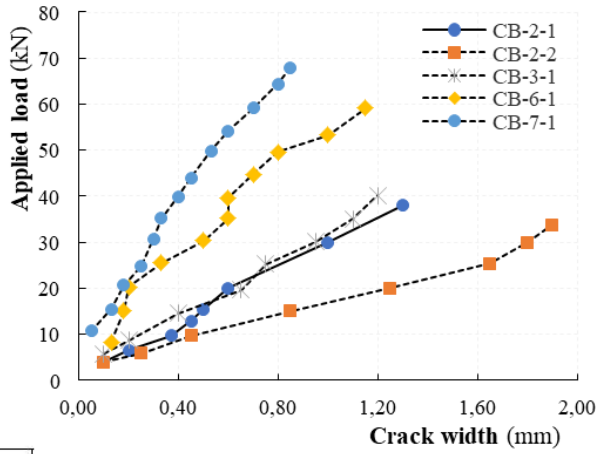

Table 2. Results of tests

Specimen	Cracking load, F_{cr} (kN)	Ultimate load, F_u (kN)	Ultimate mid-span deflection, η (mm)	Ultimate curvature at the mid-span section χ (1/mm)x 10^4	k_s (Nm^2)	DF
CB-2-1	4,90	45,76	91,65	1,1500	1750	7,33
CB-2-2	3,99	41,67	92,05	0,8576	1872	3,96
CB-3-1	5,79	58,75	90,48	0,9586	2382	4,69
CB-6-1	8,39	65,84	78,15	0,9066	2692	4,53
CB-7-1	11,78	76,34	69,57	0,7745	4144	3,77

1 N=0.225 lbf; 1 mm= 0.0394 in

4. Modeling

4.1. Proposed model

4.2. Comparison with experimental results

4.1. Proposed model

The proposed model allows for the evaluation of stresses and strains in the beam element for each cracking configuration, that is at each applied load and corresponding moment distribution. The analysis both at the serviceability and at the ultimate limit conditions is developed by a non-linear procedure.

The model was derived by a cracking analysis of a beam element subjected to bending moment higher than the first cracking one, and located between two adjacent flexural cracks, supposed to be vertical along the depth of the beam.

Two limit cracking configurations that correspond to the maximum and minimum spacing are considered; they bound all possible cracking configurations.

In the first case, the maximum crack spacing is equal to $\mathbf{l_{max}=2\ l_b}$. The slip is zero halfway between the cracks (symmetry condition) and the tensile concrete stress σ_{ct} at the extreme fiber of the halfway point of the cross-section reaches the tensile strength of the concrete $\mathbf{f_{ct}}$.

When the crack spacing is minimum $l_{min} = l_b$, the slip is still zero halfway between cracks because of the symmetry condition, whereas the tensile concrete stress at the extreme fiber of the halfway point of the cross-section is unknown but lesser than f_{ct}.

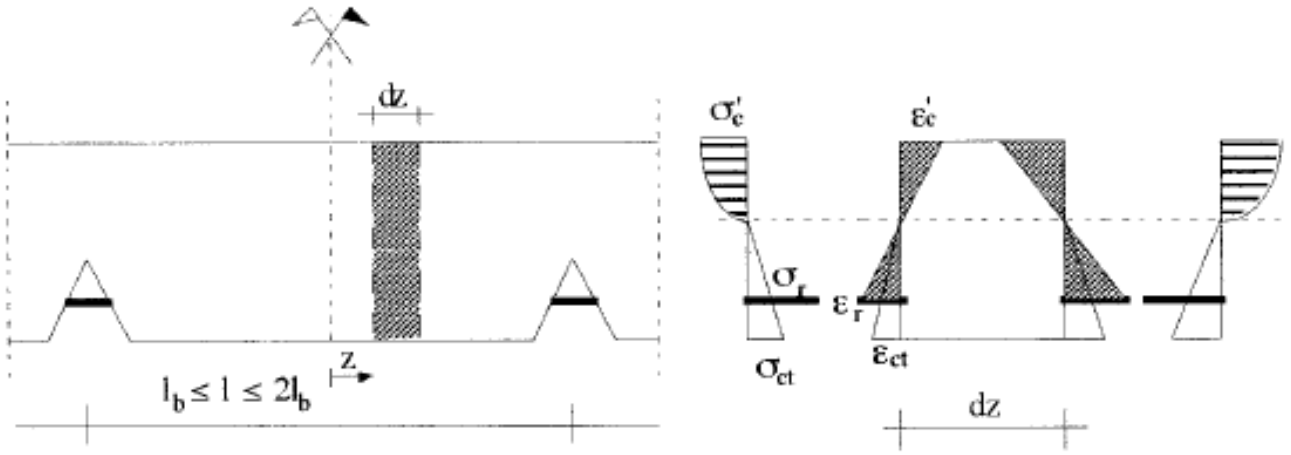

Stress and Strain Distributions at End Cross Sections of *rc* Block (Maximum Crack Spacing $\sigma_{ct} = f_{ct}$; Minimum Crack Spacing

Equations

Axial equilibrium for FRP rebars

$$\frac{d\sigma_r}{dz} = \frac{p_r}{A_r}\tau(z)$$

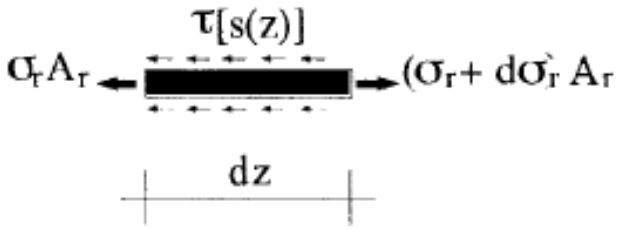

p_r, A_r= perimeter and area of the rebars, respectively; $\tau(z)$= bond stress

Compatibility conditon between two points, initially fully bonded belonging to the FRP rebars and concrete

$$s(z) = u_r(z) - u_{ct}(z) \qquad \frac{ds}{dz} = \varepsilon_r(z) - \varepsilon_{ct}(z)$$

s(z)= slip; $u_r(z)$ and $u_{ct}(z)$= displacements of the rebars and the tensile concrete; $\varepsilon_r(z)$= strain of the FRP rebars, $\varepsilon_{cr}(z)$= strain of the concrete in tension at the reinforcement level

Equilibrium conditions of the cross-section

$$\int_{\Omega_c} \sigma_c \, d\Omega_c + \sum \sigma_{ri} A_{ri} = 0$$

$$\int_{\Omega_c} \sigma_c y_c \, d\Omega_c + \sum \sigma_{ri} y_{ri} A_{ri} = M$$

Numerical procedure

A numerical procedure founded on the finite-differences method is used to solve the set of equations. The block between two consecutive cracks is subdivided in discrete elements with small length Δ_{zi}

The procedure starts evaluating the stress and strain distributions at the halfway point of the cross-section by means of the equilibrium condition (the slip is zero); therefore by means of the above equations it is possible to evaluate the stress and strain distributions at the edge cross-sections of the first discrete element contiguous to the halfway
The procedure is extended to every contiguous discrete element (the stress and strain distributions at the edge section of the i_{th} element is known , because it is evaluated at the adjacent edge section of the *i-1* element) and it halts when the concrete tensile stress becomes zero (crack opening).

Consequently

$l_b = \Sigma_{i=1,n} \Delta_{zi}$ being n the number of discrete elements, and the mean curvature of the block

$$\chi = \frac{1}{l_b} \sum_{i=1}^{n} \left(\frac{\varepsilon_{ri} - \varepsilon_{cii}}{d_i} \right) \Delta z_i$$

d_i= effective depth of the beam.

Varying the bending moment it is possible to evaluate the moment-curvature diagram of the block.

Bond-slip law

The non-linear bond-slip law proposed by Cosenza-Manfredi and Realfonzo was adopted in this analysis

$$\frac{\tau}{\tau_1} = \left(\frac{s}{s_1}\right)^{\alpha}, \quad \text{if } s \leq s_1$$

$$\frac{\tau}{\tau_1} = 1 - p\left(\frac{s}{s_1} - 1\right), \quad \text{if } s_1 \leq s \leq s_3; \tau = \tau_3 \quad \text{if } s \geq s_3$$

Type of outer surface (1)	α (2)	p (3)	τ_1 (MPa) (4)	s_1 (mm) (5)	τ_3 (MPa) (6)
Smooth rebars	0.145 (0.44)	1.87 (0.53)	1.19 (0.44)	0.26 (0.99)	0.99 (0.47)
Ribbed type	0.283 (0.56)	14.88 (1.20)	11.61 (0.34)	1.23 (1.19)	7.79 (0.60)
Grain covered	0.067 (0.81)	3.11 (0.96)	12.05 (0.09)	0.13 (0.37)	3.17 (0.22)

Deflections of the reinforced concrete beams were evaluated by the principle of the virtual work

4.2. Comparison with experimental results

The predictions of the model were compared with the experimental results and with predictions obtained by other available models, namely those provided by ACI code and JSCE code.

The comparison is reported in terms of ultimate load, moment-curvature diagrams, load-mid-span deflection curves and load-maximum crack widths curves.

Table 3. Comparison between predicted and experimental ultimate load values

Beams	Experimental P_{uexp} (kN)	Non-linear model prediction Pu(kN)	ACI model prediction P_{uACI} (kN)	P_u/P_{uexp}	P_{uACI}/P_{uexp}
CB-2-1	45,75	44,53	45,73	0,973	0,999
CB-2-2	41,67	44,53	45,73	1,069	1,098
CB-3-1	58,76	50,55	62,00	0,860	1,055
CB-6-1	65,84	61,58	68,28	0,935	1,037
CB-7-1	76,34	71,11	71,68	0,932	0,939

1 N= 0.225 lbf

The analysis of data evidences that both considered models furnish predictions in very good agreement with the experimental results.
The results of the proposed non-linear model are more conservative while the ACI model slightly overestimates experimental values.

4.2. Comparison with experimental results

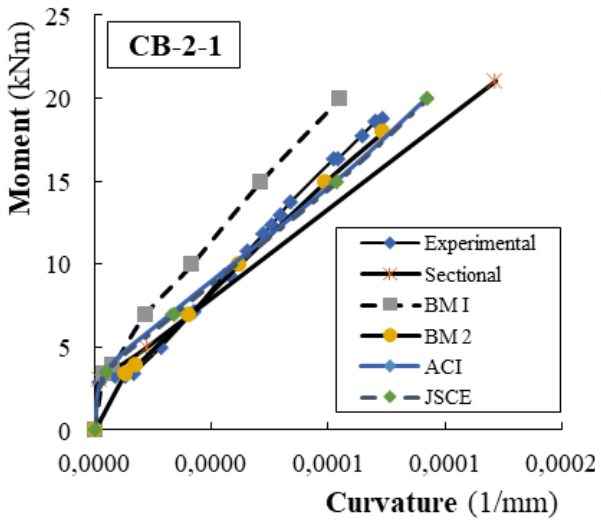

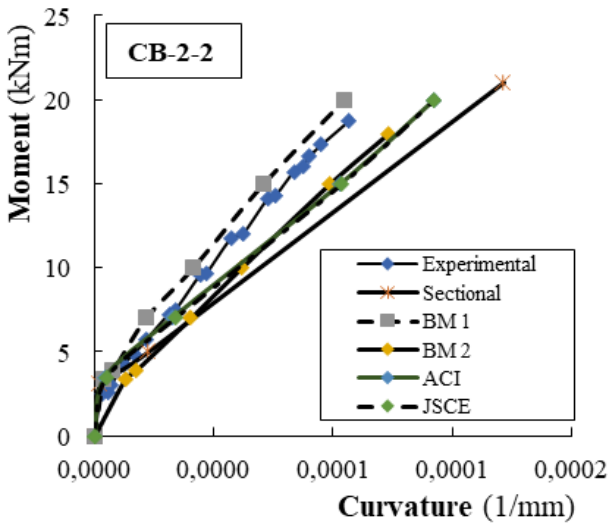

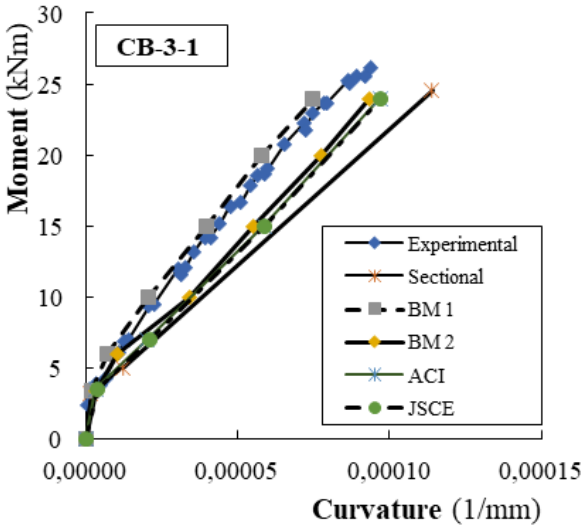

The diagrams show the comparison between experimental and predicted moment-curvature.

Predictions of the non-linear model refer to two limit cracking configurations, namely corresponding to the minimum and maximum crack spacing, and labeled as BM1 and BM2, respectively.

Predictions of the non-linear model were evaluated adopting a non-linear bond slip law.

4.2. Comparison with experimental results

The comparison shows that the BM1 and BM2 curves bound the experimental curve mainly for low values of the applied loads.

Curves corresponding to the Code models, based on the use of an "effective moment of inertia" of the cross section show a similar trend; they generally overestimate experimental values.

For all beams, the moment-curvature diagrams obtained by the "sectional approach" (perfect bond between FRP bars and concrete) overestimate the experimental results mainly for high values of the applied loads.

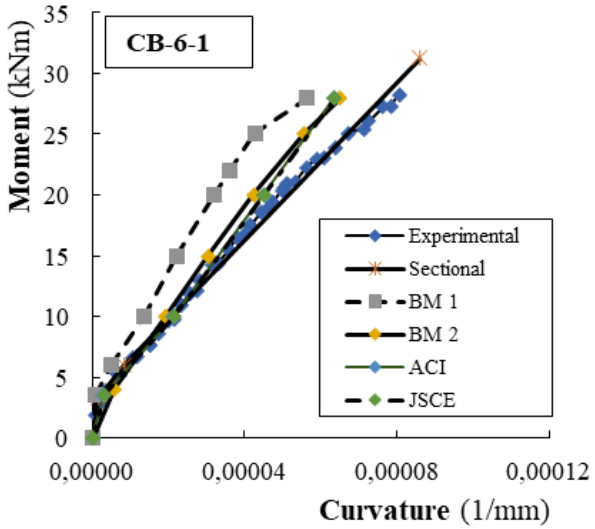

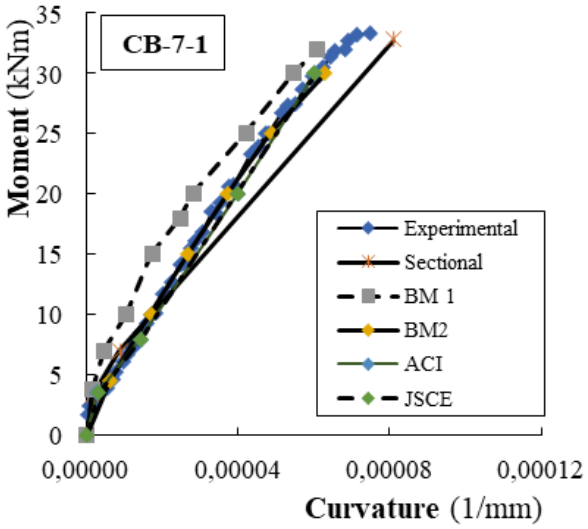

4.2. Comparison with experimental results

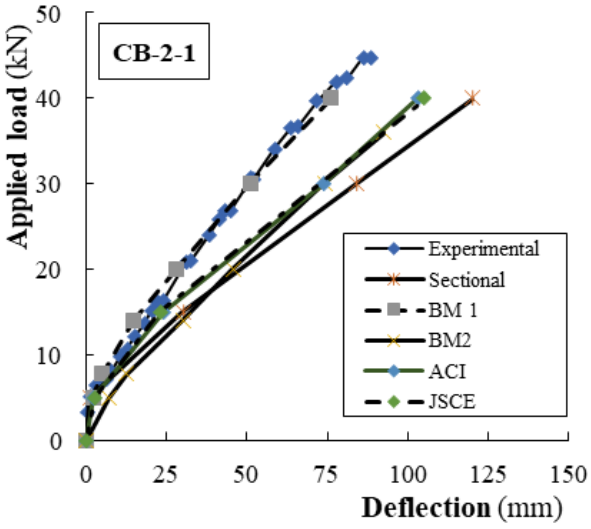

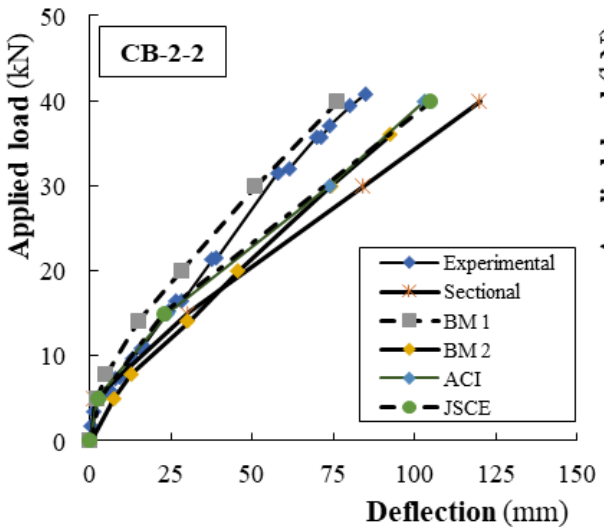

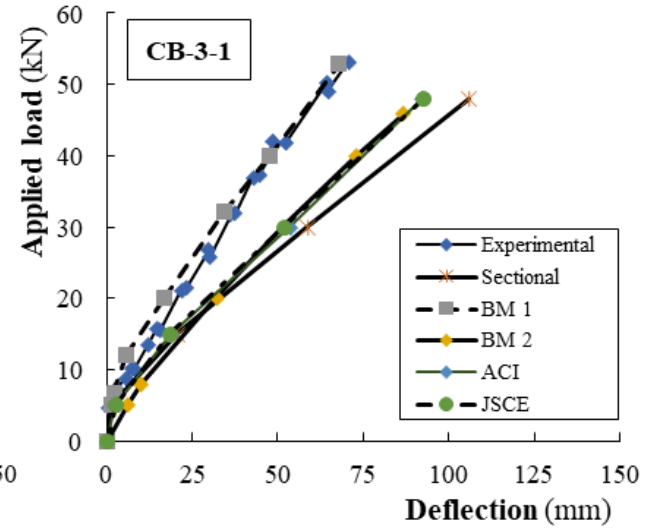

Regarding the comparison between model's predictions and experimental results in terms of load versus mid-span deflections, for beams where a flexural failure occurred, the non-linear model (BM1 and BM2 curves) is able to well predict the experimental values.

For CB-2-1, CB-2-2 and CB-3-1 beams in fact, the BM1 curves are in good agreement with the experimental ones while the BM2 curve fits well the experimental results for the CB-6-1 beam.

4.2. Comparison with experimental results

Values of deflections predicted by Code and sectional models are higher than experimental ones mainly for high load values.

For the CB-7-1 beam, for which a shear failure occurred, the experimental deflections values are higher than those predicted by the non-linear model while they are lower than those estimated by both ACI, JSCE and sectional models.

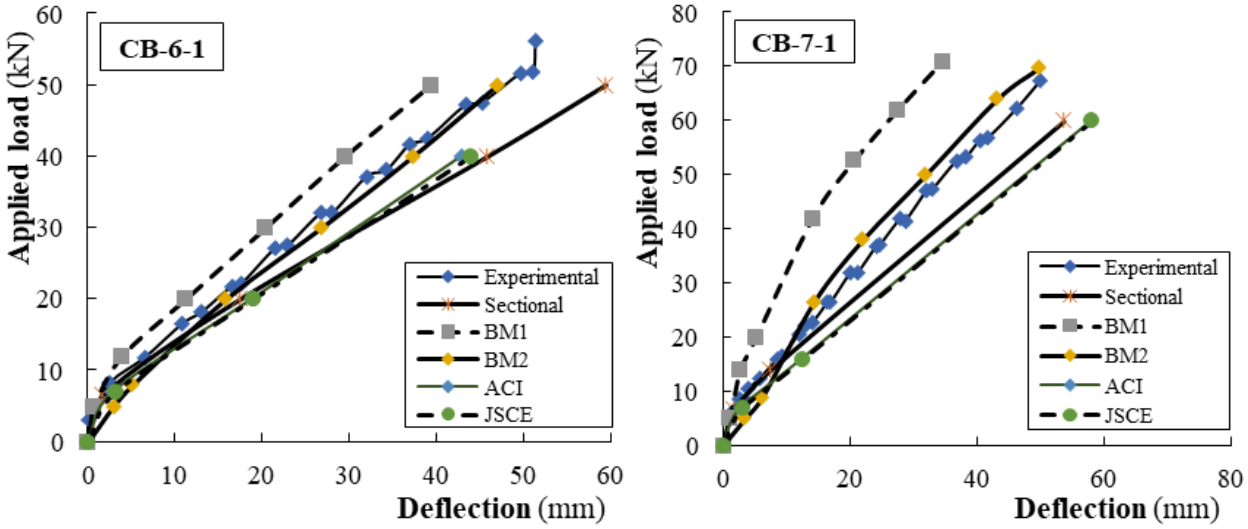

4.2. Comparison with experimental results

As evidenced in the following diagrams, predictions of the non-linear model generally overestimate the experimental crack widths for all tested beams.
The predictions provided by the ACI model are in good agreement with the experimental values, while the EC2 model underestimate the experimental values at any load level.

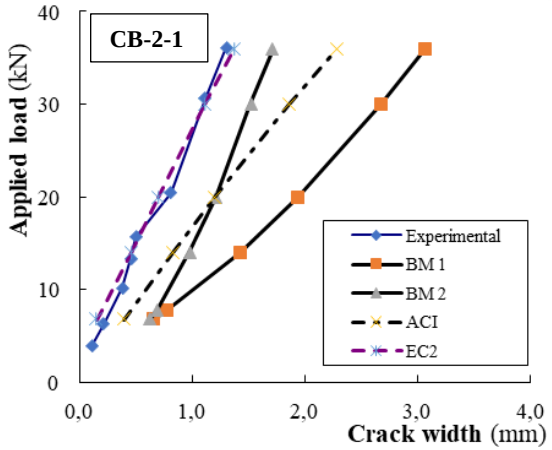

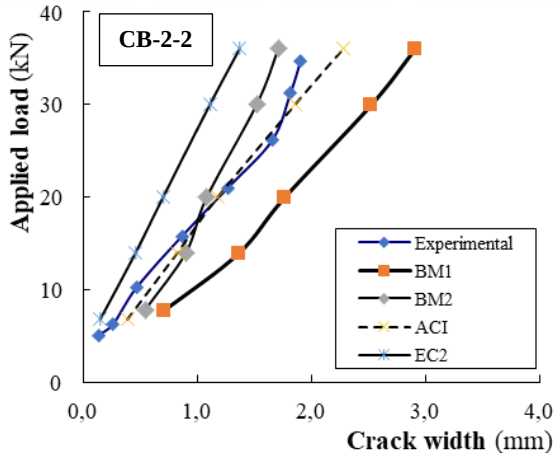

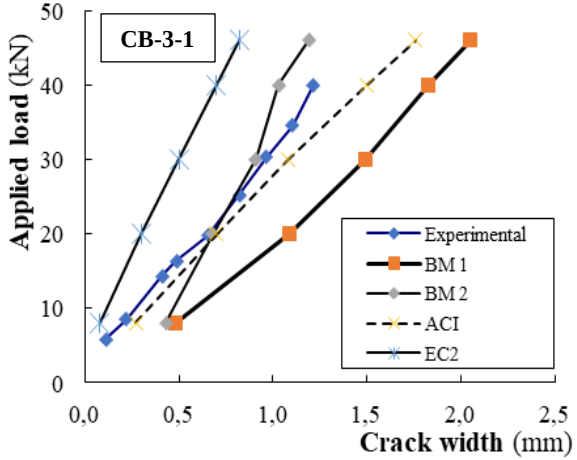

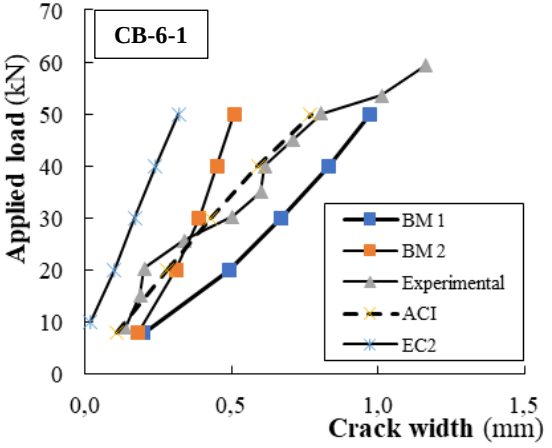

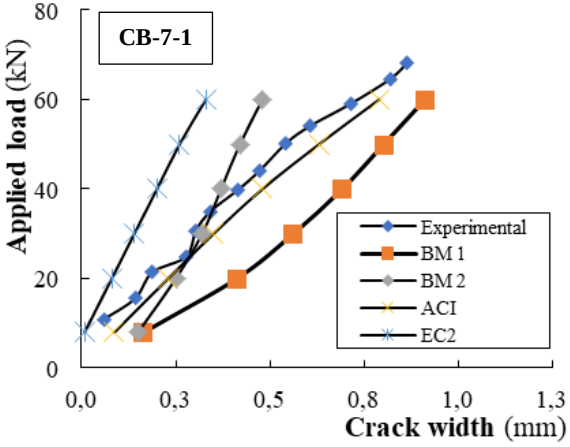

5. Open issues

5.1. Deformability

5.2. Workability

5.3. Durability

5.1. Deformability

The experimental results confirmed that the mechanical behavior of concrete beams reinforced with FRP bars is characterized by excellent performance in terms of strength and high deformability under service conditions.

The high deformability is associated with a reduced beam stiffness, resulting from diffuse cracking also characterized by high values of crack width.

Deformability and cracking, also accompanied by reduced structural ductility have been and still are addressed by researches in the field, mainly aiming to explore technological and construction solutions able to overcome these drawbacks.

5.1. Deformability

i) Among proposed solutions are those involving the use of FRP bars with surface finish configurations that can provide effective locking and increase the bond with concrete.

ii) Hybrid bar solutions obtained with the use of fibers of various types or obtained with steel bars coated with a layer of FRP (fibers +matrix) can be effective for reducing deformability and cracking, while contributing to a pseudo-ductile behavior.

iii) A promising construction solution is the use of hybrid reinforcement.The beams are reinforced by a hybrid system, consisting of FRP bars and steel bars, appropriately arranged to optimize the mechanical response of the beams in terms of strength and deformability, as well as to guarantee a higher durability.

5.2. Workability

Another issue that characterizes the use of composite bars is their workability.
The bars that are currently used are made from thermosetting resins, which have a predominant limitation: due to the brittleness of the material, once the resin has cured, the bars cannot be shaped.

The use of thermoplastic resin reinforcements would overcome the limitation of bars made with thermosetting ones. The use of these resin would allow rebar to be shaped directly on site.

However, knowledge of the mechanical properties of them is still limited; in fact, most scientific studies are based on experimental campaign and focused their attention on the mechanical characterization of the new bars present on the market.

5.3. Durability

Issues related to the mechanical behavior of concrete beams reinforced with FRP bars that need further investigations are those related to the influence of long-term effects and durability.

Excessive deformability of concrete beams reinforced with FRP bars will certainly be enhanced by the influence of viscous effects occurring in both the concrete and the matrix of the composite.

Different experimental results obtained evidence that the physical-mechanical properties of composite bars remain almost unchanged, under typical environmental conditions. On the contrary, the durability of concrete can be affected by environmental agents.

It follows that although FRP bars are characterized by high durability, concrete structures reinforced with FRP bars may not be as durable.

Similar problems may occur in beams reinforced with FRP bars exposed to high temperatures. In such case, the high vulnerability of composite bars to the effects of high temperatures may compromise the mechanical behavior of the reinforced structures.

6. Conclusions

The experimental results evidenced the main issues that characterize the mechanical behavior of FRP reinforced concrete beams*:*

i) the serviceability behavior, both in terms of cracking and deflections, and the low ductility value;

ii) all tested beams failed by crushing of the concrete in compression and their ultimate strength increases with the reinforcement ratio;

iii) an almost linear distribution of strain along the section depth was recorded;

iv) the flexural stiffness of the tested beams at the cracked stage increases with the reinforcement ratio while crack widths were decreasing with the reinforcement ratio.

Models currently provided by Codes furnish reasonable predictions both for serviceability and ultimate conditions.

The analytical investigation gives evidence that an accurate and reliable modeling is needed to well predict the behavior of the FRP reinforced concrete beams accounting for the real constitutive law of materials and their interaction (FRP bar-to-concrete bond*).*

The proposed non-linear model could be extended to deepen the improved performances deriving from new and less explored technical solutions and materials.

Thanks for your attention!